Endolymphatic structures in headshields of the osteostracan genus *Tremataspis* (Agnatha) from the Silurian of Estonia

Tiiu Märss[a*], Mark V. H. Wilson[b] and Mart Viljus[c]

[a] Department of Geology, Tallinn University of Technology, Ehitajate tee 5, 19086 Tallinn, Estonia
[b] Department of Biological Sciences, University of Alberta, Edmonton, Alberta T6G2E9, Canada; mvwilson@ualberta.ca
[c] Department of Mechanical and Industrial Engineering, Tallinn University of Technology, Ehitajate tee 5, 19086 Tallinn, Estonia; mart.viljus@taltech.ee

*Corresponding author, tiiu.marss@taltech.ee

Abstract. Details of the endolymphatic structures are described for the first time in the headshields of the osteostracan genus *Tremataspis* from the Silurian of Estonia. Tiny platelets, here termed covering platelets, are located within the openings of the endolymphatic duct. The details of their shapes and arrangements differ among the four studied species. In *Tremataspis schmidti* Rohon and *Tremataspis milleri* Patten, the covering platelets are usually arranged in an oval or circular shape around the opening of the endolymphatic duct. These species can have smooth, flat covering platelets at the mouth of an irregularly funnel-shaped aperture in the dorsal shield; the funnel often has a posterior extension. In *Tremataspis rohoni* Robertson and *Tremataspis mammillata* Patten, a distinct circular arrangement of platelets does not occur; instead, their funnel was capped with a few (2–3) smooth, flat covering platelets. The funnel of *T. milleri* sometimes has a long postero-lateral extension, while that of *T. mammillata* can have a short extension; no extensions of the funnel have been observed in *T. schmidti* or *T. rohoni*. The diameter of the pores in the covering platelets is larger than that of the pores in the superficial layer of the headshield and much larger than the diameter of the pores in the porous fields (these are thin perforated bony septa subdividing the sensory canals horizontally into lower and upper parts). In *T. milleri,* the larger pores are located on the side of the covering platelets that is closer to the body midline. The discovered system of covering platelets possibly functioned as a sieve for allowing in suitable grains of material and preventing material that is too fine or too coarse, or not sufficiently dense, from entering the inner ear.

Keywords: endolymphatic structures, *Tremataspis,* Osteostraci, Wenlock, Ludlow, Silurian, Estonia.

INTRODUCTION

Osteostracans from the Silurian of Saaremaa Island, Estonia, are well known and have been examined many times since their first description more than 165 years ago (Eichwald 1854). The most recent monographic work was about Silurian osteostracan biodiversity based on the study of their articulated headshields, scales, and various microscopic fragments (Märss et al. 2014). That osteostracan collection also included a headshield fragment bearing a pair (left and right) of external endolymphatic structures with a complicated morphology of a more medial duct opening surrounded by tiny platelets, here termed covering platelets, along with a posterior extension, all within the limits of a larger asymmetrical funnel. This discovery was interesting because the external endolymphatic structures and their functions in

osteostracans are not known and had yet to be studied in detail. Moreover, their characteristics are often excluded from systematic and phylogenetic analyses of osteostracans. Therefore, the osteostracan collections at the University of Tartu and Tallinn University of Technology were studied, the better-preserved specimens were sorted, and scanning electron microscope (SEM) studies of the area behind the medial dorsal field were carried out. It was found that the distinctive covering platelets were not rare but were usually invisible without SEM examination.

HISTORICAL REVIEW

Information about the openings of the endolymphatic ducts (also known as endolymphatic pores) in early vertebrates includes studies on these structures in osteostracans

by Stensiö (1927, 1964), Janvier (1985), and Sahney and Wilson (2001). Endolymphatic duct openings have also been reported in acanthodians (Watson 1937; Sahney and Wilson 2001), most of which are now often regarded as stem-group chondrichthyans (e.g., Dearden and Giles 2021, fig. 7). Such duct openings are also present in modern chondrichthyans (e.g., Hanson et al. 1990; Mills et al. 2011).

Watson, studying the acanthodian *Climatius reticulatus* (Watson 1937, p. 54, fig.1; pl. 5, fig. 2), described and drew a minute foramen for the endolymphatic duct as "a little to each side of the mid-line of a pair of rather larger bones which meet one another in a straight transverse suture. On the left side in this suture there is a very minute foramen whose border lies mainly in the posterior bone; the opening is less clearly seen on the right" (Watson 1937, p. 134). This differs substantially from our *Tremataspis* in the shape and size of the surrounding plates. Watson (1937) added that the *ductus endolymphaticus* also opened on the top of the head in elasmobranchs.

Stensiö (1964, fig. 116) illustrated a part of the semicircular division and part of the canal for the endolymphatic duct in *Tremataspis mammillata.* Janvier (1985, fig. 22A) published drawings and descriptions of the same feature in *Tremataspis*. Sahney and Wilson (2001) studied representatives of five vertebrate groups, including osteostracans, from the Delorme Group, Lochkovian, in the Mackenzie Mountains of Canada. They examined granular labyrinth infillings composed of sand-sized particles, which they discovered posterior to the orbits in all the examined species of osteostracans, acanthodians, and putative chondrichthyans, but not in heterostracans or thelodonts. They found that the labyrinth infillings consisted at least partly of exogenous grains (ibid., p. 660). Those authors suggested that the morphology of the endolymphatic duct probably allowed selective entrance of larger or denser particles (Sahney and Wilson 2001), as occurs in extant chondrichthyans (Hanson et al. 1990). The exogenous material passed from the environment, through the endolymphatic duct, and into the labyrinth of the inner ear (Sahney and Wilson 2001; Märss et al. 2022), where it functioned for hearing and balance detection.

In the present paper, we discuss two possible modes for such selective entrance of particles: either large pores in the covering platelets functioned as a sieve for appropriately sized particles, or a single endolymphatic duct opening of appropriate size within the structure restricted the particle size. We describe the details of endolymphatic structures in four species of the genus *Tremataspis* (Osteostraci), including the surrounding otic elevation, the funnel, the covering platelets, the opening of the endolymphatic duct, the size of the endolymphatic duct itself, and the diameter and number of pores in the covering platelets. We used pore diameters and pore density of the sensory canal system in the headshield to identify species.

We show also that even microscopic fragments of fossils are valuable because they allow interpretations of details and provide clues about the func- tion of organs.

MATERIAL AND METHODS

Material

The collections of the Natural History Museum (NHM) at the University of Tartu and the Department of Geology at Tallinn University of Technology (TUT) contain thousands of *Tremataspis* specimens, from which we selected nearly 50 specimens for this study and examined 29 specimens using the SEM. The NHM holds E. Bölau's collections of *Tremataspis*, which he used for his study of *Tremataspis Sinnesliniensystem* (Bölau 1951), and A. Luha's collection, both obtained from the Himmiste Quarry. Specimens from the Viita Quarry, Vesiku Brook and Elda Cliff (Fig. 1) stored at the TUT were collected by T. Märss and her fieldwork colleagues. The large dolostone blocks in the Särghaua fieldstation were not studied. Of the 29 specimens selected for SEM study, seven belong to *Tremataspis schmidti* Rohon (GIT 846-1, GIT 846-3, GIT 846-4, GIT 846-6, GIT 846-8, GIT 846-9, GIT 846-11), six to *Tremataspis milleri* Patten (GIT 846-2, GIT 846-5, GIT 846-7, GIT 846-13, GIT 502-435, GIT 502-443), two to *T. rohoni* Robertson (GIT 846-10 with doubt, GIT 846-12) and fourteen to *Tremataspis mammillata* Patten (TUG 1025- 32, TUG 1025-342, TUG 1025-358-1, TUG 1025-358-2, TUG 1025-567, TUG 1025-586, TUG 1025-722, TUG 1025-728, TUG 1025-803, TUG 1025-831, TUG 1025-840, TUG 1025-1041, TUG 1030-24, TUG 1030-27).
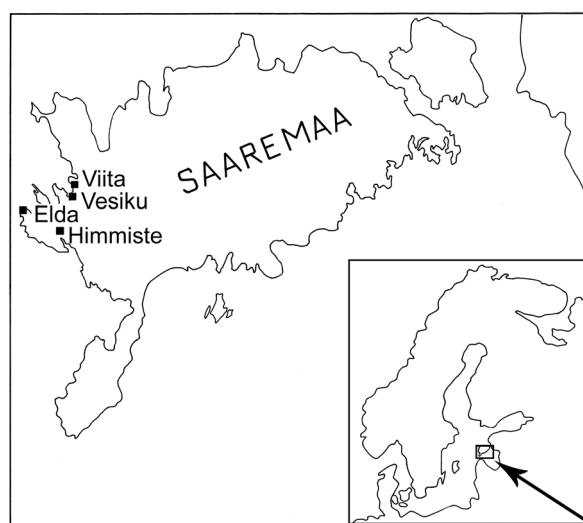

Fig. 1. Location of Viita, Vesiku, Elda and Himmiste outcrops on Saaremaa Island in Western Estonia.

Table 1. Measurements of pores in the headshields of the holotypes of four *Tremataspis* species from Estonia (Märss et al. 2014; D: taken from Denison 1947).

Taxon	Tubercle No. on headshields	Density of headshield pores (approx. No. of pores per mm^2)	Diameter of headshield pores (µm)
T. schmidti	4	100	20–25 (D: 21–25)
T. milleri	6–8	200	15–20 (D: 14–16)
T. mammillata	20 or more	15	30–35 (D: the same)
T. rohoni	>10; 14 in holotype	30 (D: denser than in *T. mammillata* but wider than in *T. milleri* or *T. schmidti*	<20 (D: 30–32)

Three specimens listed as *T. mammillata* revealed pineal and nasohypophysial microstructures briefly described herein.

Stratigraphically, the specimens originate from the bonebed layer in limestones at Vesiku Brook, Vesiku Beds, from micro-laminated dolostone in the Viita Quarry, Viita Beds, and Elda Cliff, Kuusnõmme Beds, Rootsiküla Regional Stage, Homerian, Upper Wenlock, middle Silurian, and from micro-laminated dolostone in the Himmiste Quarry, Himmiste Beds of the Paadla Regional Stage, Gorstian, Ludlow, upper Silurian.

Methods

Available materials consisting of smaller pieces of rock were studied. We were unable to move large stone blocks from the Särghaua fieldstation to Tallinn for studying with light and SEM microscopy. Cleaning of the finest platelets around the external endolymphatic openings was complicated because of the risk of breaking or losing those platelets. We attempted to clean the platelets using sharpened needles, but both the opening and platelets were too small relative to the needle. We tried dissolving the dolostone by adding acid drop by drop, but without any success, since the platelets disintegrated and floated apart. An ultrasonic bath, used earlier to prepare thelodont scales, also disintegrated the platelets. A few specimens that had soft, clayey sediment in the opening or between the platelets were cleaned with fine brushes. In the end, we decided to work with the finest needles, but on the condition that we did not risk losing any more platelets. The drawback was that we did not always achieve as clean a surface of the platelets as we would have liked.

Line drawings, which we used to show the details under discussion, were made on separate layers directly from SEM images using Adobe Photoshop.

A Zeiss EVO MA15 microscope with a Lanthanum hexaboride electron source was used for SEM imaging. The applied accelerating voltage was 10 kV and the working distance was usually 10–15 mm. The samples were ion sputtered with Au-Pd alloy to ensure electrical conductivity of their surface. The samples contained entrapped gases (because of their relatively large size and porous material), which made it difficult to achieve the required high vacuum in the SEM specimen chamber. The optimal solution was to insert a batch of samples into the microscope chamber at the end of a working day and take the images as the first job the next day.

To identify the species of *Tremataspis*, we counted the number of pores per mm^2 on the headshield of specimens and measured pore diameters in the headshield behind the median dorsal field and between or near the duct openings (Tables 1–3). Then, elements of the external endolymphatic structures (otic elevation, funnel, duct opening, posterior extension of funnels, covering platelets, and covering platelet pores) were described for each of the four studied species of *Tremataspis*.

Tremataspis perforata Märss et al., 2014, was established on fragmentary material that did not have any preserved endolymphatic structures and was therefore not included in this study. Among the other nominal species of *Tremataspis*, *T. simonsoni* Rohon has been treated as a junior synonym (Robertson 1938), and three other nominal species – *T. patteni* Robertson, *T. scalaris* Robertson, and *T. panderi* Robertson – are almost identical to *T. mammillata* and have been synonymized with the latter by Denison (1947).

TERMINOLOGY

In this section we explain the terms we have applied; most abbreviations are given in Fig. 2. The external endolymphatic structure is a term that includes all the external endolymphatic elements discussed here, and a representative example is illustrated diagrammatically in Fig. 2H. It includes a shallow funnel on either side of the midline, often with a narrow posterior extension, variable numbers and shapes of covering platelets, which might include sieve pore (or sizer pore) platelets, and the opening of the
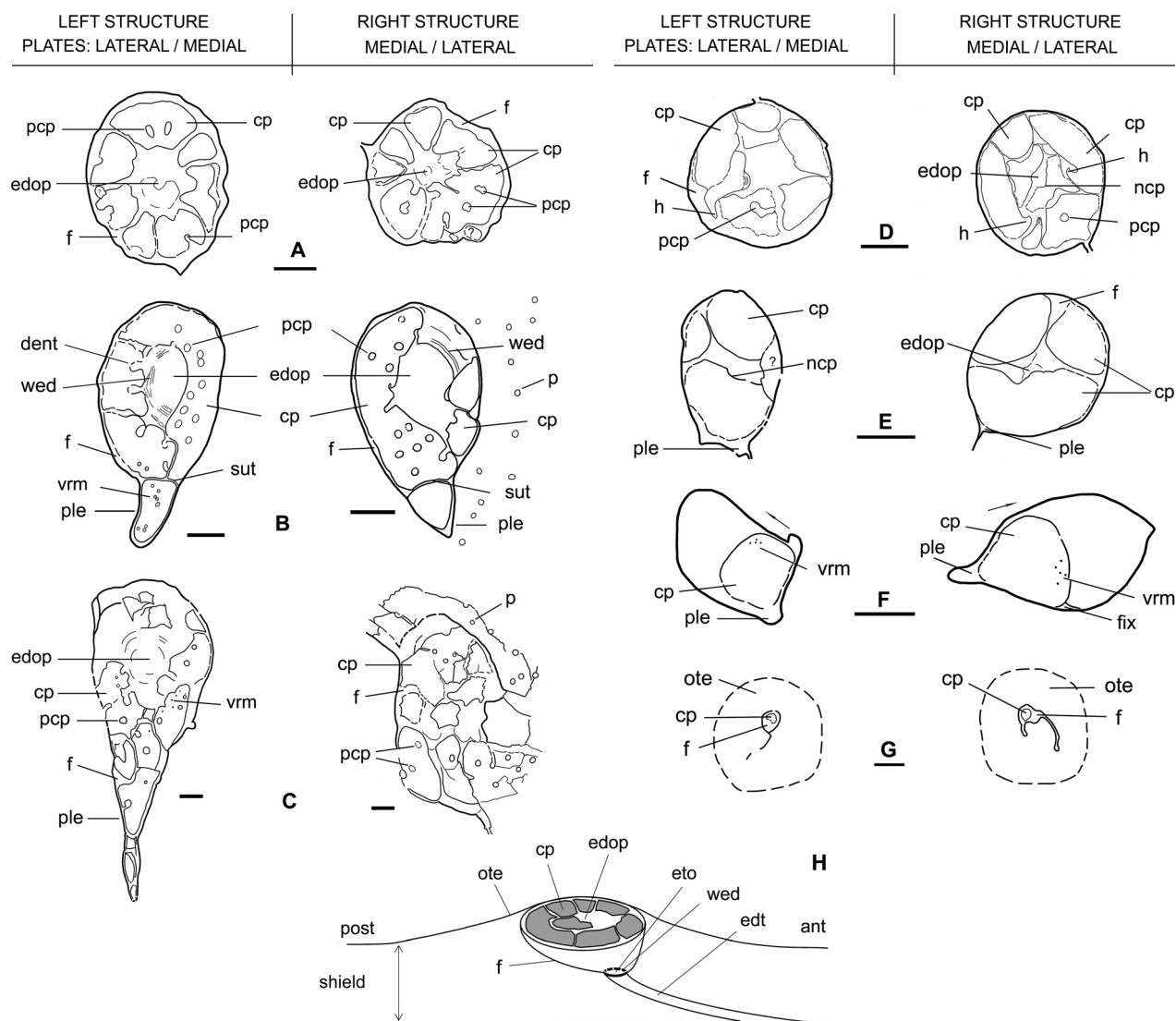
Fig. 2. Line drawings of endolymphatic structures. **A**, *Tremataspis schmidti* Rohon; **B–D**, *Tremataspis milleri* Patten; **E**, *Tremataspis rohoni* Robertson; **F**, **G**, *Tremataspis mammillata* Patten; **H**, diagram of a representative external endolymphatic structure in *Tremataspis*. Scale bar = 100 µm (A–F); 400 µm (G).

Abbreviations for Figures 2–9: ant, anterior; cap, very small cap-like platelet; cp, covering platelet; dent, dentate margin of a covering platelet or shield; dmf, dorsal median field; edop, endolymphatic duct opening among covering platelets; edt, endolymphatic duct tube; eto, endolymphatic tube opening; f, funnel; fix, fixing aid?; fr, fibrous, rope-like structure; h, hook-like end of a covering platelet; ncp, notch in a covering platelet; ote, otic elevation above the surrounding shield; p, pore of the sensory canal system; pcp, large pore in a covering platelet; pin, pineal structure; ple, posterior/postero-lateral extension; ppf, pores of a porous field/perforated bony septum; r, ridges; sc, sensory canal; sut, suture and/or discontinuity; t, any tube except an endolymphatic duct tube; vrm, microbial vermicular traces; wed, wall of endolymphatic duct.

duct itself within the funnel leading into the endolymphatic duct tube that is directed toward the labyrinth, all of these being located on or within a larger otic elevation on the surface of the shield.

The endolymphatic duct tube is a lumen surrounded by a bony wall and narrowing deeper into the headshield. Its dorsal end opens into the funnel and through it extrinsic grains passed in and endolymph or seawater passed both

out and in, as in sharks and ratfishes (Sahney and Wilson 2001; Chapuis et al. 2022). In sharks, the endolymphatic duct opens into a broad, shallow fossa, which is a single indentation or depressed area of the posterior chondrocranium, surrounding both openings of the endolymphatic duct (Popper and Fay 1977).

The external openings of the endolymphatic duct have been called pores in some fishes, including osteostra-

cans (e.g., Sahney and Wilson 2001) and sharks (Popper and Fay 1977). However, the word "pore" is not sufficiently precise to be used for osteostracans such as *Tremataspis* because the same specimen of a species can have at least four sizes of small pores, presumably with different functions. The following types of pores can be distinguished in *Tremataspis*: 1) pores of the sensory canal system of the headshield, 2) pores of porous fields (= perforated laminae; = perforated septa) with the diameter of micro-apertures of the septum being 3–4 μm for *T. schmidti* (Märss et al. 2014, p. 91), 3) small openings on the surface of the covering platelets within the funnel, and 4) tiny openings left by microbial organisms (may include pre- or post-mortem fungal or bacterial damage). These are all in addition to the openings of the endolymphatic duct.

A fossa is a large depression or hollow, often around a medial or paired duct opening (e.g., Janvier 1985), referring to the more anterior circumnaso-hypophysial fossa of osteostracans, or to the parietal or endolymphatic fossa of sharks (Popper and Fay 1977; Maisey 1985, fig. 1A, C). The endolymphatic fossa of sharks encompasses both left and right duct openings.

The function of the endolymphatic funnel in *Tremataspis* appears to be to guide extrinsic grains into the endolymphatic duct, allowing only appropriately sized grains to reach the duct tube itself.

Covering platelets lie within the funnel surrounding the opening of the endolymphatic duct, but also within the funnel's postero-lateral extension, if present (e.g., *T. milleri*). They consist of simple tiny platelets in a corona- or wreath-like arrangement, or in an oval ring around the opening, or arranged in a parquet-like pattern, covering the whole funnel, or on two levels resembling the leaf shutter or iris diaphragm of older cameras.

The extension of the funnel is the posteriorly (or postero-laterally) narrowing area of both the funnel and its covering platelets. It does not occur in all specimens/species. Its function is unknown.

The wall seen inside the duct opening surrounds the lumen of the endolymphatic duct.

The otic elevations are paired, round to oval elevations around the funnels that include the opening of the endolymphatic ducts. Their shapes depend on the main structure, the width and length being measured across the elevation, from foot to opposite foot.

An otoconium is a minute, transparent, calcite crystal with well-developed faces secreted within a labyrinth, where it is often mixed with exogenous mineral particles (Rojo 2017; Coad and McAllister 2020). Those of Cyclostomata and Chondrostei are usually 1–50 μm in diameter, with some otoconia up to 250 μm (Nolf 1985).

Extrinsic mineral grains incorporated into the otolith mass via the endolymphatic duct (e.g., Sahney and Wilson 2001) are called otarenae (Bond 1979; Kasumyan 2004;

Rojo 2017; Coad and McAllister 2020), meaning "ear sand". Otarenae occur in many chondrichthyans; they usually occur in addition to otoconia produced endogenously within the labyrinth of the animal, and both types are ultimately combined into a "composite otolith," cemented by organic matrix, in which the grains remain distinct (Kasumyan 2004). In our case, the dolomite crystals found at the mouth of the endolymphatic duct are about 10–20 μm in diameter, which presumably could have entered the duct. However, in the extant shark *Heterodontus portusjacksoni*, only otarenae and no otoconia are reportedly found (Mills et al. 2011). Another recent discovery reports polycrystalline otoliths in some chondrichthyans, superficially similar to the calcium carbonate otoliths of bony fishes, but composed mostly of apatite in the chondrichthyan examples (Schnetz et al. 2019).

RESULTS

General features of *Tremataspis*

External endolymphatic structures in *Tremataspis* are located posteriorly and somewhat laterally to the median dorsal field. In some specimens, their location is anterior to the posterior margin of the median dorsal field. The long axis of the endolymphatic structures is not strictly antero-posterior but can be slightly oblique. The configuration of these structures can be roundish, elongate, or asymmetrical. The funnel in some specimens can have an elongate extension posteriorly or postero-laterally, and its length seems to depend on the taxon. The tiny covering platelets partly or completely roof the funnels but can also block the duct opening; the covering platelets can be in one or two layers. The density and diameters of the pores of the sensory canal system in the headshield, as well as the diameters of the funnels and the pores of the covering platelets, are given in Tables 2 and 3.

Description of endolymphatic structures in specimens of the four species

Tremataspis schmidti Rohon

The morphology of the covering platelets in these specimens is homogenous: short platelets lie in a circular or oval shape around the openings of the endolymphatic ducts, within the funnel; as a rule, pores in the covering platelets are relatively large. The otic elevations are weak.

In specimen **GIT 846-1** (Figs 2A left and right; 3A, B), both endolymphatic structures are well preserved. This specimen belongs to *T. schmidti* based on the density of the shield pores (100–120), the diameter of the shield pores (14–16 μm) (Table 2), and the four sets of tubercles

Table 2. Numerical data on headshield pores and pores in covering platelets and funnels of three species – *Tremataspis schmidti* Rohon*, T. milleri* Patten, and *T. rohoni* Robertson. Tubercles were countable in only two specimens.

Taxon	Collection No.	Tubercle No.	Density of shield pores (approx. pores/mm^2)	Diameter of shield pores, µm	Diameter of funnels, µm; l: left and r: right funnel	Diameter of pores in covering platelets, µm
T. schmidti	GIT 846-1	4 short rows	100–120	14–16	l: 431 × 363 r: 362 × 361	30 × 15 elongate
T. schmidti	GIT 846-3	4	112	13–15	l: 136 × 245 r: 122 × 188	?
T. schmidti	GIT 846-4		105	?	?	?
T. schmidti	GIT 846-6		100	12–17	r: ?719 × 618	13–17
T. schmidti	GIT 846-8		120	14–19	l: 534 × 607 r: 577 × 747	11–16
T. schmidti	GIT 846-9 (juvenile?)		82–88	10–13	l: 467 × 372	12–14
T. schmidti	GIT 846-11		115	12–16	r?: 875 × 720	15–17
T. milleri	GIT 502-435 "wound"		118	11–19, mainly14		
T. milleri	GIT 502-443		192–218	14–20, mainly16	l: ?608 × 312 r: 525 × 290	17–23; 20–24
T. milleri	GIT 846-2		205	12–16	l: ?1500 × 600 r: 920 × 485	17–25
T. milleri?	GIT 846-5		>200	12–15	l: 389 × 339 r: 419 × 340	14–20
T. milleri	IT 846-7		200	12–14	l: 297 × 297 r: 316 × 293	17–20; hook 30
T. milleri	GIT 846-13		150	10–17	300 × 394; 514 with branches	24
T. rohoni?	GIT 846-10		110	10–15	330 × 360	15–20
T. rohoni	GIT 846-12		30–45	12–15	l: 268 × 167 r: 267 × 228	notch 40

on the shield. The contour of the funnels is roundish to oval, and covering platelets are distinctly separated from the shield. Seven small platelets are in one ring, and a crescentic structure is in the middle, on the duct opening in the left endolymphatic structure (Fig. 3A), and as an indistinct bony element in the right one (Fig. 3B). The right structure bears one larger, undivided covering platelet in the lower right part of the funnel. Some platelets of the structures mirror each other (see Fig. 2A). Individual large pores in the covering platelets are highly elongate (measured as 30 × 15 µm). The shield surface around the endolymphatic structures is smooth, without otic elevations.

Specimen **GIT 846-6** (Fig. 3C, right structure), with its pore density **(**ca 100 p/mm^2) and shield pore diameter

(12–17 µm) fits with *T. schmidti* (Table 2). It has an oval configuration with a vertical crack anteriorly and it is slightly laterally compressed. The groove separating the covering platelets from the headshield is relatively wide. The platelets are in two ovals, one nested inside the other, and one tiny, a nearly ring-like structure is also close to the center. The number of covering platelets in the outer oval is 5–6? (two large, arch-like platelets and 3–4 small ones posteriorly), and the number in the inner oval is 5 (one arch-like platelet and 4 smaller ones). The diameter of the pores in the covering platelets is 13–17 µm.

Specimen **GIT 846-8** (Fig. 3D, E) has a pore density of 120 p/mm^2 and a shield pore diameter of 14–19 µm (Table 2). The funnels have an oval configuration with margins partly notched and partly simply broken. The

covering platelets have a convex surface. The pores in the covering platelets and the headshield are of similar diameter. The left structure (Fig. 3D) bears distinct intact platelets in the outer oval, and additionally 3–4, mostly broken platelets in the middle. The right structure (Fig. 3E) has six platelets in a regular outer ring, plus two transitional ones posteriorly, and two in the middle. The pore diameter in the covering platelets is 11–16 μm. The posterior margin of both funnels has a transition from indentations to a smooth shield surface. Such a feature is seen in many other specimens as well. Figure 3H (*T. milleri* GIT 502-435) shows a healed wound in the dorsal headshield with incisions and indentations at the margins. Such evidence was needed to evaluate whether configuration at the posterior margin of the funnels was natural or the result of breakage.

The shield surface of **GIT 846-9** (Fig. 3F, left structure) is partly broken, but the wreath-like formation of the covering platelets is well recognizable. The outer measurements of the "wreath" are 400 × 400 μm. The calculated density of headshield pores is approx. 82–88 p/mm^2 and the pore diameter is 10–13 μm. The pore diameter in the covering platelets is 12–14 μm (Table 2); thus, the pore diameters in the platelets and shield differ very little. Next to the wreath at the bottom of the image, there is a loss of platelets. The preserved set shows six platelets in a ring and one broken platelet in the middle. There is some free space for the endolymphatic duct opening in the center. This structure is also characterized by notches at the margins of the covering platelets. Some platelets slightly cover the neighbouring ones, giving the impression of overlapped/overlapping margins.

Specimen **GIT 846-11** (Fig. 3G) is *T. schmidti* as proved by the small number of tubercles on the headshield, the density of pores in the shield (ca 115 p/mm^2), and the shield pore diameter (12–16 μm). The pore diameter in the covering platelets is 15–17 μm (Table 2). The left endolymphatic structure (the right structure is not preserved) is oval, and the shield margin around the funnel is rather uneven, especially posteriorly. The medially placed covering platelet is semicircular and long, while the number of laterally placed platelets remains uncertain (2 or 3?). In the middle there is a tiny platelet with a lateral notch, stuck in the endolymphatic duct opening. The porosity of the covering platelet is different from the other specimens in this group. Here, the diameters of the pores in the covering platelet and in the headshield are similar, but the pore density in the platelet is higher than in the headshield, which is the opposite situation compared to that in other specimens of *T. schmidti*.

Specimen **GIT 846-3** (Figs 3I, L). This is one of the few specimens to have a preserved dorsal shield showing tubercles, four in number, a trait that was used to identify *Tremataspis schmidti* Rohon, even though the values of

its shield pore density (112 p/mm) and pore diameter (13–15 μm) slightly differ from those given for the species by Märss et al. (2014) (see Table 2). Endolymphatic structures are located far posterior to the posterior margin of the dorsal median field. The longer axis of the endolymphatic structures inclines anteriorly 25–30 degrees towards the body midline. The otic elevations are weak.

Both funnels have tiny processes postero-laterally, but both funnels lack covering platelets; presumably these were lost during preservation or erosion. The left funnel is partly filled with soft sediment, hindering its examination.

The entire right-side structure is complicated and not well understood. It is in two separate parts (Fig. 3I): the main, relatively large funnel anteriorly (top left of the image), and the smaller, more distal funnel-shaped opening posteriorly (bottom right of the image). The latter has a somewhat flattened bony element with an opening in the middle, which continues posteriorly by a tube, and with loops on both sides, perhaps of parasitic origin (Fig. 3L).

Specimen **GIT 846-4** (Figs 3J, K) is *Tremataspis schmidti* from Bölau's collection. The superficial layer of its headshield has been removed during an earlier study, but some areas remained, and were used for pore density calculation (105 pores/mm^2) and species identification. The endolymphatic openings are situated immediately posterior to the posterior extremity of the short and roundish remains of the median dorsal field (Fig. 3J). Both openings of the endolymphatic duct have a roughly similar contour, wide and arcuate anteriorly and narrower and more elongate posteriorly, possibly forming impressions of postero-lateral extensions (Fig. 3J). The endolymphatic ducts themselves incline anteriorly. They occur with a smooth, internal, relatively thick-walled surface, except for rare pits (Fig. 3K). The bottom of the right structure is filled with platy bone fragments.

Tremataspis milleri Patten

Endolymphatic structures of this species are a heterogenous group in terms of the shape, size, and pattern of both the funnels and the covering platelets. The covering platelets can be in one distinct ring, divided into shorter lengths around the endolymphatic duct opening, or covering the whole funnel. The covering platelets can occur on one or two levels. The margins of the funnels and/or platelets can be smooth or uneven. There are few large pores per platelet, or the margin of the posterior platelet bears hooks forming notches.

Specimen **GIT 502-443** (Figs 2B, 4A–C) is a piece of a *Tremataspis* headshield. The pores in the dorsal headshield are rather densely distributed (192–218 pores per mm^2) as counted in three regions posterior to the median dorsal field and between the endolymphatic structures (Table 2). The diameter of the headshield pore
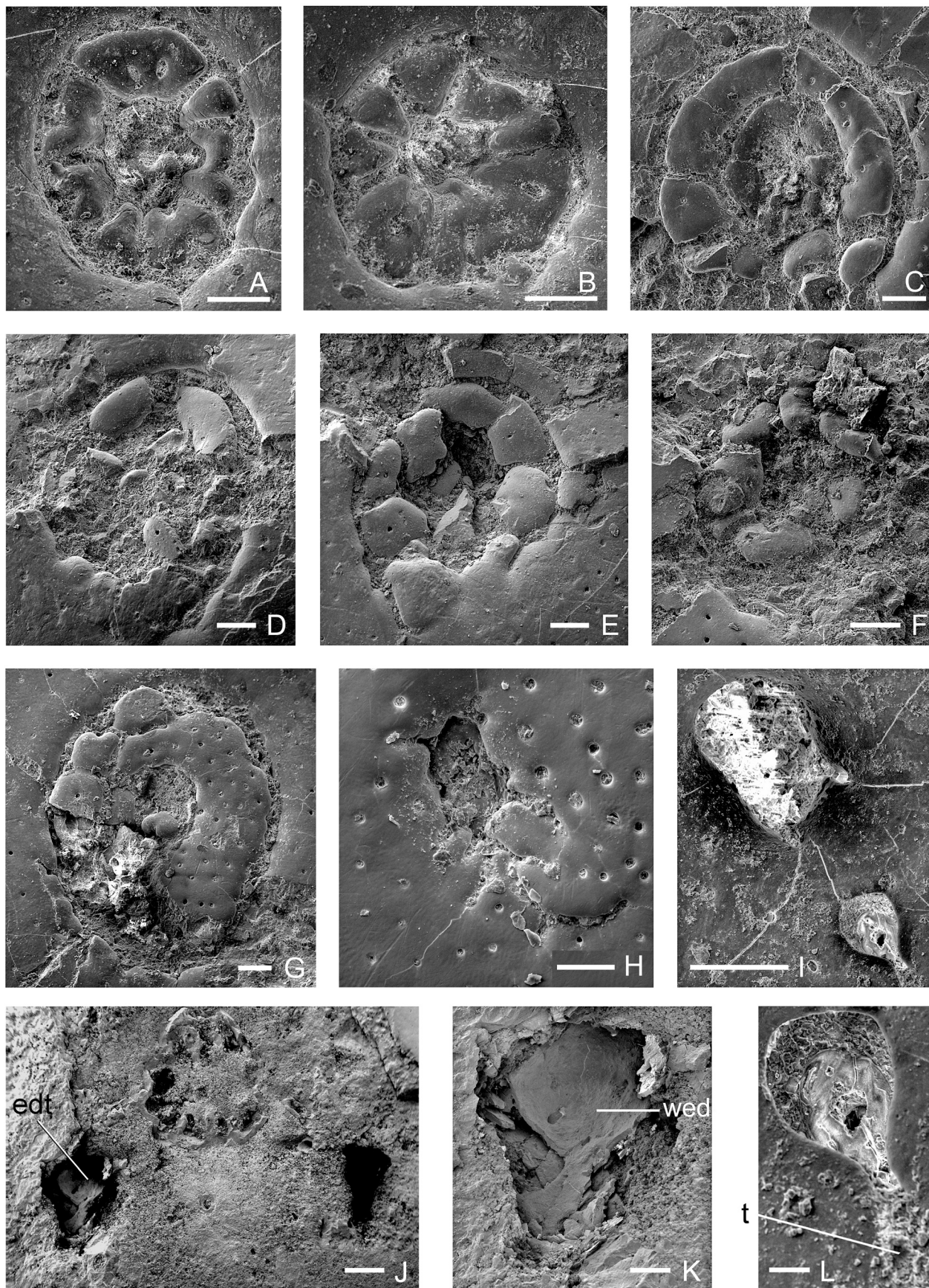
is 14–20 μm, mainly 16 μm. All these numbers indicate the identification as *T. milleri*. The slightly medially tilted left-side structure (Fig. 4A, B) is well preserved, while the right-side one (Fig. 4A, C) is straighter antero-posteriorly and has laterally lost a few small covering platelets. The contour of the funnel is oval, with a posteriorly narrowing extension. Left and right funnels are similar in shape and asymmetry. The inner margin on the lateral side of the funnel is serrated, and the contour of the external duct opening is oval. The pores in the covering platelets are about twice as large as the pores in the headshield. All visible covering platelets of this specimen seem to have been immobile. The otic elevation follows the contour of the funnel and narrows near the posterior extension; its surface is somewhat abraded.

The left endolymphatic structure of **GIT 502-443** (Figs 2B left, 4B). The maximum length of the left funnel is 608 μm and the maximum width is 312 μm across the widest oval part (Table 2). Its narrowing posterior extension is 50 μm wide at its middle. The funnel has three covering platelets of different sizes and shapes, jointly forming an oval band; the posterior extension holds the fourth platelet. The oval band has a natural longitudinal suture posteriorly. The covering platelets surround (partly covering) the medial endolymphatic duct opening, which is 200 μm long and about 100–115 μm wide. The lateral covering platelets have a dentate inner margin. No large pores occur in these platelets. On the opposite side, the covering platelet is built differently, as it lacks dentation and has a smooth inner margin. The platelet's surface has relatively large pores with a diameter of 20–24 μm (double-pore 40 μm in length), which are larger than pores of the headshield surface given in Table 2. These pores are also deep, with a porous membrane inside. The mouth of each pore is gently convex while those of the headshield surface have a more right-angled margin. Some of the small pieces of angular debris on the left side between the covering platelet and the headshield have tiny pores, which are even smaller than those in the porous fields. Due to the slight tilt of the structure, the wall of the endolymphatic duct inside (in the light part beneath the dentated margin) can be seen.

The right endolymphatic structure of **GIT 502-443** (Figs 2B right, 4C). This structure is slightly smaller than the one on the left; the funnel has a maximum length of 525 μm and maximum width of 290 μm across the oval part. Its posterior process is differently shaped than the left structure; it contains a triangular covering platelet that is 100 μm wide and only slightly longer than its width. The ovate medial endolymphatic duct opening is approximately 200 × 125 μm. The largest, porous, medial covering platelet has a pore diameter between 17–23 μm; its inner margin has two indents and two natural sutures separating this platelet from the neighbouring ones, one anteriorly and the other postero-laterally on the right side. On the lateral side are two smaller covering platelets, while the antero-lateral area of the funnel lacks any platelet, but here the internal surface of the wall of the endolymphatic duct is exposed.

Specimen **GIT 846-2** (Figs 2C, 4D–F) is another shield fragment of *T. milleri* Rohon, with a pore density of 205 p/mm², and a shield pore diameter of 12–16 μm. The external endolymphatic structures are positioned far anteriorly in relation to the posterior point of the dorsal median field (Fig. 4D). The contours of the left and right funnels differ strongly, with the posterior extension present only in the left structure. The covering platelets are different in both size and configuration. The transition from some covering platelets to the shield of both structures is smooth, without any suture. The otic elevations around both structures follow the contours of the funnels and are narrow and abraded.

The left endolymphatic structure (Figs 2C left, 4E) has an anteriorly ovate contour, but posteriorly a long and strongly sharpened extension. The length of the whole structure is 1500 μm and the maximum width is 600 μm. The endolymphatic duct opening is recognizable in the left structure, in the middle of its widest area. It is roundish, weakly marked by the edges of a few platelet fragments. The covering platelets in the funnel, as much as preserved, are smooth and of different sizes around the duct opening. An aberrant bone structure is continuous with the headshield on the left lateral side; it is not a separate covering platelet. The next platelet posteriorly is a similar case. Such smooth transition between covering platelet and shield is also described below for the right-side endolymphatic structure. The suture between the covering platelets of the lateral and medial sides is well seen shortly before the narrowing of the extension. The posterior extension is covered with small platelets, which

Fig. 3. A–G, **I–L**, *Tremataspis schmidti* Rohon, SEM images of external endolymphatic structures; **H**, *Tremataspis milleri* Patten. **A**, **B**, left and right structures, GIT 846-1; **C,** right structure, GIT 846-6; **D**, **E**, left and right structures, GIT 846-8; **F**, left structure, GIT 846-9; **G**, left structure, GIT 846-11; **H**, an image of a healed wound, included herein for comparison with normal marginal features of funnels, GIT 502-435; **I**, **L**, complicated structure of two right openings in GIT 846-3 (**L** is a close-up of the lower right element in Fig. 3I); **J**, **K**, left and right openings, GIT 846-4 (**K** is a close-up of the left element in Fig. 3J). *Locations:* GIT 846-1, GIT 846-3, GIT 846-8, GIT 846-11, Elda Cliff, loose material; GIT 846-6, GIT 846-9, Elda Cliff, bed II, Kuusnõmme Beds; GIT 846-4, Viita Quarry, Viita Beds, Rootsiküla Regional Stage, Homerian, Upper Wenlock; GIT 502-435, Himmiste Quarry, Himmiste Beds of Paadla Regional Stage, Gorstian, Lower Ludlow. Scale bars = 100 μm (A–I); 500 μm (J); 200 μm (K); 20 μm (L). *Abbreviations*: edt, endolymphatic duct tube; wed, wall of an endolymphatic duct; t, any tube except an endolymphatic duct tube.
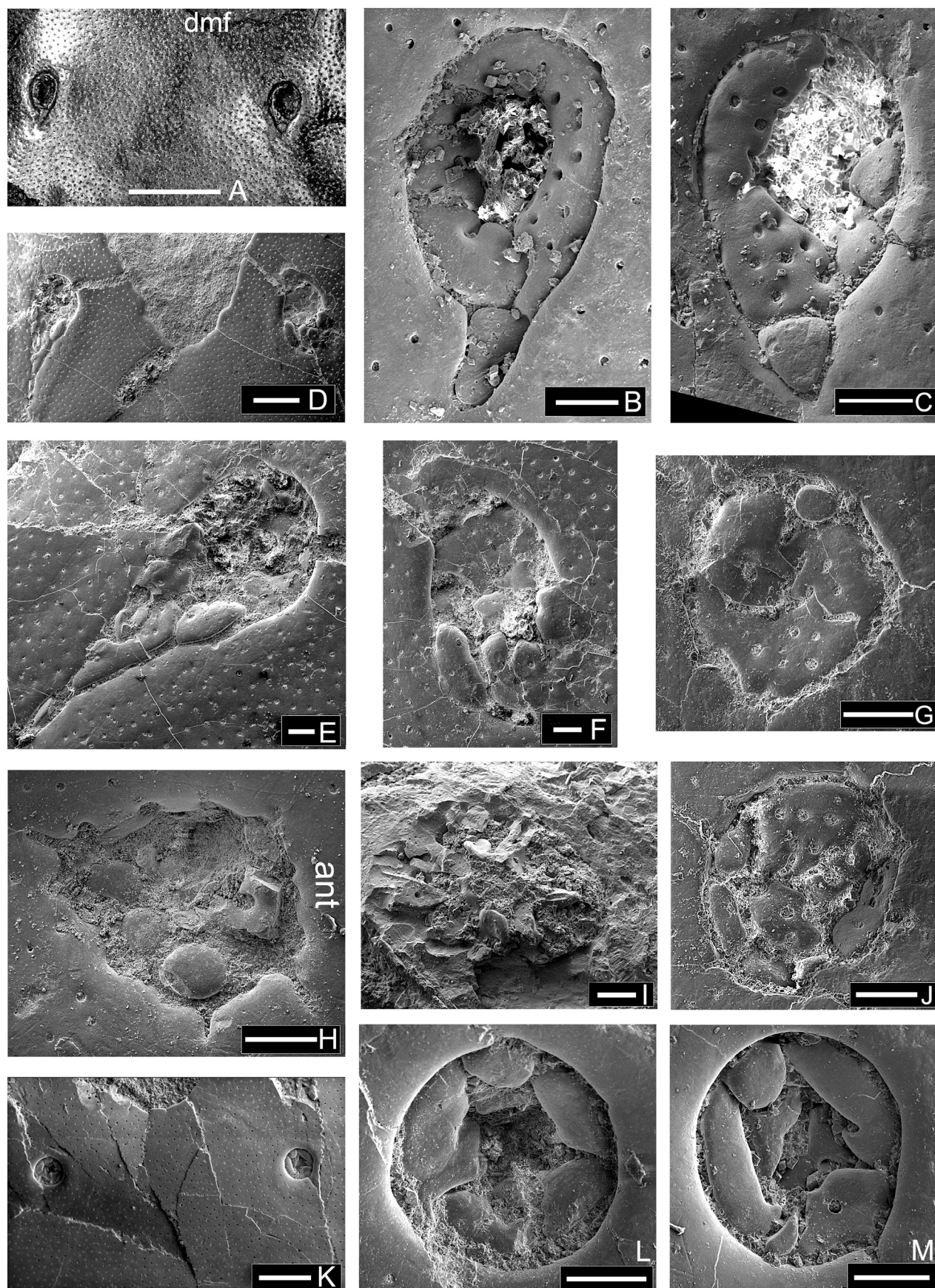
have one to two slightly larger pores, the largest located posteriorly on both sides of the suture with a pore diameter up to 23 μm. Up to 6–7 openings of microbial origin with a diameter of 6–10 μm were counted in the covering platelets.

The right endolymphatic structure (Figs 2C right, 4F) is shorter than the left one, being about 920 μm long and 485 μm wide. The contours of covering platelets in the middle of the funnel are indistinct; the surface of the relatively large covering platelets anteriorly and of the two convex, seemingly thick, small platelets more posteriorly is smooth and flat; these, in turn, are followed by four digit-like outgrowths. Part of these outgrowths is continuous posteriorly with the headshield, but the left medial one is separated from the shield. Each "digit" bears one or two pores, which are larger than the headshield pores. The placement of the median duct opening is not clear. The shape of the posterior covering platelets resembles the elements ("tongues") of healed wounds in some other *Tremataspis* (see Fig. 3H).

Specimen **GIT 846-5** (Fig. 4G, J) has covering platelets that are distinctly separated from the shield around the perimeter. The pore density and pore diameter of the headshield fit with *T. milleri*, while the pores in the covering platelets are only slightly smaller than in other *T. milleri* specimens; they are, however, 2–3 times larger than in the headshield. The pore diameter and density in the covering platelets are higher than in other *Tremataspis* species (with the exception of GIT 846-11 *T. schmidti*, Fig. 3G). The small number of covering platelets is similar to the condition of *T. rohoni specimens* (Fig. 5A–C below), but the pore size and density do not fit with this species. The covering platelets are of different sizes, the left funnel has one large and one cap-like platelet, and the right funnel has one large, two medium and four small platelets, including a cap-like one. The platelets (or only one large + a cap) have a smooth surface covering the entire funnel, and the endolymphatic duct opening is not visible.

Specimen **GIT 846-13** (Fig. 4H, I), despite some deviations in shield pore density (density 150 p/mm^2, diameter 10–17 μm, and platelet pore diameter 24 μm; Table 2), this specimen might still be *T. milleri*.

The left funnel (Fig. 4H) is roughly triangular, with all margins notched around it. Inside the funnel there are three small, roundish covering platelets with convex and smooth surfaces, lacking pores, and three? fragments, one of which bears a large pore at its medial edge. This is an interesting structure because of the notched margin around the funnel. We speculate that if the covering platelets are too small to be pierced by pores, the margin of the shield becomes notched and assumes the filtering function.

The right funnel (Fig. 4I) exposes the radial pattern of the middle layer if the superficial layer of the shield is broken away. Three well-preserved platelets (at least three on the left side) have a concave surface close to the duct opening. The sensory canals on the left side are very wide. A fibrous, rope-like structure laterally surrounds the area where the platelets are usually located.

GIT 846-7 is a specimen of *Tremataspis milleri* Rohon (Figs 2D, 4K–M) because of the headshield pore density, which is 199 pores per mm^2, but also because of the very small diameter of the headshield pores (12–14 μm) and the slightly larger pores in covering platelets (17–20 μm) (Table 2). The contours of the funnels are nearly circular, though one is slightly more elongate. The covering platelets are small to medium in size; the smallest platelets anteriorly in both funnels resemble caps (as, for example, in Fig. 4G). The covering platelets of both left and right structures are well preserved and are present on two to three? levels in this specimen. Their disposition on different levels resembles the leaf shutter or iris diaphragm of older cameras. Some covering platelets of both structures have strange hooks with deep notches in their posterior corners, which could substitute for the pores of the covering platelet. The single large pores in the covering platelets (one per funnel) resemble those of *T. rohoni* (GIT 846-10, Fig. 5C below). The otic elevation is low, not very distinct, and is abraded around the funnels.

The left endolymphatic structure of **GIT 846-7** (Figs 2D left, 4L). The length and width of the left funnel are 297 × 297 μm. A single relatively small covering platelet and a partial platelet beneath it are exposed anteriorly; next on this lateral side is a pair of connected, somewhat longer platelets, and a platelet with an irregular configuration is located posteriorly. This platelet has two pore-like incisions with widened parts (approx. 20–30 μm in diameter). On the opposite, medial side of the left-side structure are two slightly elongate platelets with well-preserved natural margins. The two platelets on the upper

Fig. 4. *Tremataspis milleri* Patten, SEM images of external endolymphatic structures. **A**, a light photograph of the dorsal headshield with the posteriormost part of the median dorsal field and a pair of external endolymphatic structures, GIT 502-443; **B**, **C**, SEM images of left and right structures of **A**, respectively; **D–F**, endolymphatic structures of very complex appearance, GIT 846-2; **G**, **J**, very small funnels with covering platelets but without any observable medial opening, GIT 846-5; **H**, **I**, funnel with small roundish platelets on the left structure, and funnel with a broken superficial layer uncovering the radial structure on the right structure, GIT 846-13; **K–M**, very well preserved endolymphatic structures in two layers, the covering platelets resembling the shutter or aperture plates of old cameras, GIT 846-7. *Locations:* A–C, GIT 502-443, Bonebed layer in the Vesiku Brook locality; Vesiku Beds; D–F, GIT 846-2, Elda Cliff, loose material; G, J, GIT 846-5, Elda Cliff, bed II; H, I, GIT 846-13, Elda Cliff, bed IV; K–M, GIT 846-7, Elda Cliff, bed IV; Kuusnõmme Beds of Rootsiküla Regional Stage, Homerian, Upper Wenlock, Lower Silurian. Scale bars = 1 mm (A); 500 μm (D, K); 100 μm (B, C, E–J, L, M). *Abbreviations*: ant, anterior; fr, fibrous, rope-like structure; dmf, medio-dorsal field.
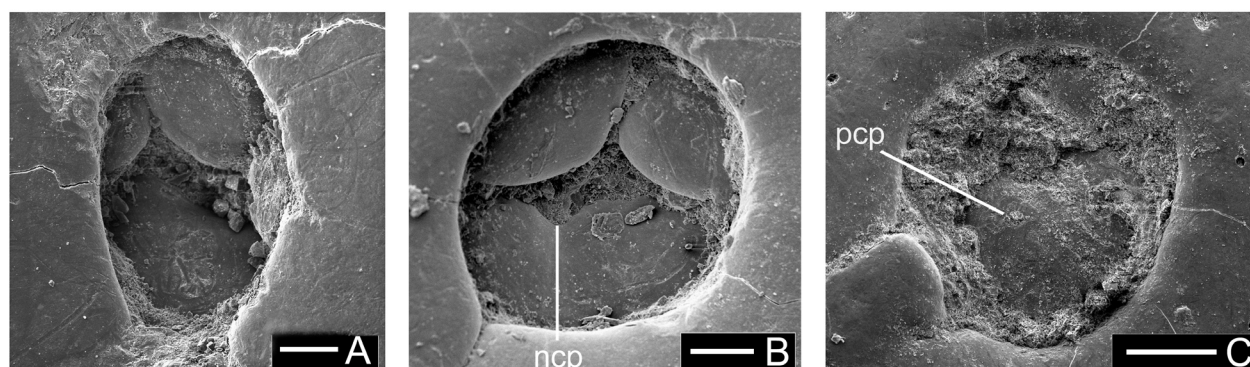
Fig. 5. A, **B**, *Tramataspis rohoni* Robertson; **C**, *Tremataspis rohoni*? Robertson. *Locations*: A, B, GIT 846-12; C, GIT 846-10, Elda Cliff, bed IV; Kuusnõmme Beds of Rootsiküla Regional Stage, Homerian, Upper Wenlock, Lower Silurian. Scale bars = 50 μm (A, B); 100 μm (C). *Abbreviations*: ncp, notch in a covering platelet; pcp, large pore in a covering platelet.

level have strange hooks, which possibly served some kind of interlocking function, at the same time leaving some space for movement.

The right endolymphatic structure of **GIT 846-7** (Figs 2D right, 4M). The length and width of the right funnel are 316 × 293 μm. There are five covering platelets on the upper level: a small one, two long ones, and two of medium size. Two covering platelets with a complicated T-shaped configuration are on the lower level, leaving some space between them, with a kind of widening in the center formed by two notches. It looks as though the lower-level platelets bridge the gaps between the upper-level platelets. The orientation of the larger platelets on the two levels differs by about 35 degrees. The hooks are very well expressed in the posterior parts of the long platelets. A single pore, about 20 μm in diameter, is present in the postero-lateral platelet.

Tremataspis rohoni Robertson

Specimens of *Tremataspis rohoni* are very rare, with only two specimens studied herein. The covering platelets are relatively large, smooth and flat, and three in number – a trait that can be considered a characteristic feature of the taxon. The presence of 1–2 pores per platelet, or a notch at the platelet's margin, has also been found here, and in that they differ from *T. mammillata*, which has no pores in covering platelets (or not found so far).

Specimen **GIT 846-12** (Figs 2E, 5A, B) has a headshield's pore density of 30–45 p/mm^2, which is between the values for *T. mammillata* and *T. schmidti-T. milleri*. The funnels are of different configurations, the left one (Figs 2E left, 5A) being oval but the right one (Figs 2E right, 5B) roundish. Both funnels are equipped with just a few (three) covering platelets. Covering platelets are smooth and flat, with their visible margins gently turned viscerally, and their outer margins hidden beneath the shield. The posterior platelet in the right funnel has a notch medially; the platelet in the left funnel has sediment on the corresponding spot and no notch is visible. No pores are seen in platelets of either funnel.

Tremataspis rohoni? Robertson

Specimen **GIT 846-10** (Fig. 5C) has the following characteristics: rare and small pores of the headshield, pore density ca 110 p/mm^2, pore diameter of the headshield 10–15 μm, and pore diameter of the covering platelet 15–20 (30?) μm. Only one (or two?) pores are seen on the posterior covering platelet. The pore density of the headshield is too high in *T. rohoni*, but more similar to that of *T. schmidti*; the diameter of the pores of the covering platelets is closer to that of *T. milleri* and both also have smooth and flat covering platelets, but *T. milleri* has numerous such pores, while *T. rohoni* has only a few; *T. mammillata* has no pores (i.e., not discovered herein). Due to the very scanty material, we avoid identifying the specimen, but provide its description.

The contour of the funnel is nearly circular, with maximum width to length ratio of 330–360 μm. One covering platelet has a pore diameter of 17–18 μm. The covering platelet pore is half the size larger than those in the headshield. The shield margin around the funnel has two notches postero-laterally, forming a "tongue" between them. The covering platelets are smooth and flat and very large; the number of covering platelets might be two, or maximum three, all being on the same level. The otic elevation is weak.

Tremataspis mammillata Patten

Funnels are normally roundish to oval, or irregular; postero-lateral extensions are common; one smooth, fixed,

relatively large, slanting covering platelet and a horizontal small cap-like roundish covering platelet are present in the funnel; covering platelet pores are absent (not found so far). Data on the pores of *T. mammillata* are given in Table 3.

Specimen **TUG 1025-32** (Figs 2F, 6A–C) is *Tremataspis mammillata* with a pore density of 15 p/mm², and a diameter of 30–50 µm, measured between funnels (Märss et al. 2014 gave 30–35 µm, but it might depend on where on the headshield it was measured). The length of the left funnel (Figs 2F left, 6B) is 285 µm, and that of the right one (Figs 2F right, 6C) is 373 µm, with its width of 200 µm. The axes of the funnels are asymmetrical, the longer axis of the left funnel is at 35 degrees and the right funnel at 75 degrees in the opposite direction to the body midline. Both funnels have a short posterior process and another anteriorly or laterally; both funnels have a single, relatively large, smooth and flat, slanting covering platelet on their posterior side inclining anteriorly or antero-laterally, the left one at a steeper angle. The right platelet has a short process possibly for fixing the platelet inside the funnel. No large pores were detected in these single covering platelets; still, both platelets have fine openings at their deeper margin, likely parasitic vermicular traces. The otic elevations around both funnels are distinct; the direction of the long axis of the elevations copies that of the funnels, with the angle between the directions of the funnels being ca 102 degrees. The elevations are ap-

proximately 700 × 900 µm (left) and 900 × 800 µm (right) in size.

Specimen **TUG 1030-24** (Fig. 6D–F) has a pore density of 10–12 p/mm² and a pore diameter of 30–43 µm. The funnels are somewhat tetragonal in shape, the one on the left (Fig. 6E) having a process antero-laterally, while the one on the right (Fig. 6F) lacks a distinct process. Both funnels have one large, smooth, slanting covering platelet – the left platelet with a process seemingly for fixing the position of the platelet on its medial side. This might be similar to what Denison (1947, p. 354) wrote concerning the attachment of a plate. The wall of both endolymphatic ducts has a laminated construction anteriorly. The covering platelet in the right funnel lacks its upper layers; only a fibrous basal layer remains. Otic elevations of both structures are distinct.

Specimen **TUG 1025-840** (Figs 2G, 6G, H) is identified as *Tremataspis mammillata* based on a pore density of 13 p/mm² and pore diameter of 35–36 µm. The funnels lie relatively far posterior to the posterior margin of the median dorsal field. The left funnel has a tiny posterior extension (Figs 2G left, 6G), and a smooth and flat, partly broken covering platelet at a greater depth. The right funnel (Figs 2G right, 6H) has one horizontal cap-like covering platelet displaced from its concavity on the shield margin and rotated around its midpoint. In this funnel there is space for fitting at least one more covering platelet. There is a finger-like part

Table 3. Numerical data on headshield pores and pores in covering platelets and funnels of *Tremataspis mammillata* Patten

Taxon	Collection No.	No. of tubercles	Density of shield pores (No. of pores per mm²)	Diameter of shield pores, mm	Diameter of funnel, µm; l – left and r – right funnel	Diameter of pores in covering platelets, µm
T. mammillata	TUG 1025-840	24	13	35–36	l: 215 × 332 r: 219 × 301	?
T. mammillata	TUG 1030-24		10–12	30–43	l: 239 × 303 r: 166 × 202	–
T. mammillata	TUG 1025-803		15	37–40	?, complicated	?
T. mammillata	TUG 1025-32		15	30–35	l: 285 r: 373 × 200	–
T. mammillata	TUG 1025-831		13	38–48	?	–
T. mammillata	TUG 1025-728		13	30–40	177 × 258	?
T. mammillata	TUG 1025-722		11	20–25	l: 132 × 142 r: 100 × 124	?
T. mammillata	TUG 1025-358-1		10–14	?	?	?
T. mammillata	TUG 1025-358-2		12–15	?	?	?
T. mammillata	TUG 1025-567		11–13	30–32	?	?
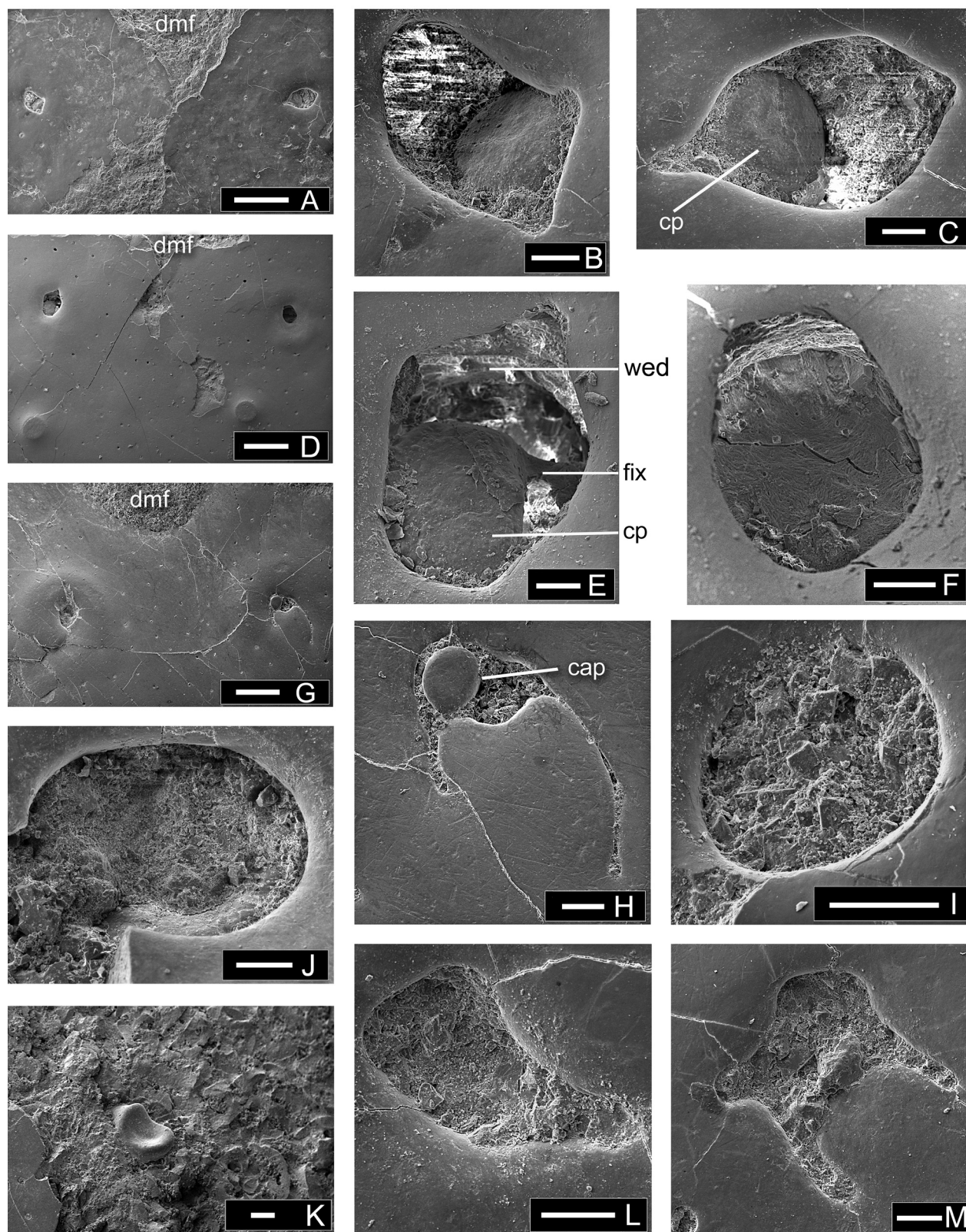
posteriorly, separated from the shield by two fissures, meaning that this area might have been repaired with a "tongue"-like extension of the headshield. No pores were observed in the platelets. The otic elevations are very distinct (Figs 2G; 6G) and roundish in shape around both endolymphatic structures. The measurements of both otic elevations were taken in two directions and were approximately 1350 × 1340 μm (left) and 1340 × 1460 μm (right).

Specimen **TUG 1025-722** (Fig. 6I) is identified as *Tremataspis mammillata* Patten, with a rare shield's pore density of 11 p/mm^2, and a rare shield's pore diameter of 20–25 μm). This is the thinnest shield (ontogenetically youngest) of the specimens in the set. The funnels are very small and roundish, and situated rather far back from the posterior end of the median dorsal field. The measurements of the funnels are 132 × 142 μm for the left funnel, and 100 × 124 μm for the right one. The left funnel is filled with dolomite crystals CaMg(CO$_3$)$_2$ and argillaceous debris (Fig. 6I), as revealed by the analysis of the chemical content. The right funnel has a crescentic bone inside it. The otic elevations are distinct.

Specimen **TUG 1025-728** (Fig. 6J, K) has a shield's pore density of 13 p/mm^2. The left-side structure (Fig. 6J) is fairly well preserved; the shield margin around the oval funnel is incomplete but the preserved part is gently downturned. Internally, the funnel reveals a narrow rim posteriorly, and fragments of smooth covering platelets in the middle. The headshield at the right structure (Fig. 6K) is broken, but there is a suggestion of some radial bone pattern of the middle layer at the place where the endolymphatic structure was. Here, an atypical concave platelet is present.

Specimen **TUG 1025-803** (Fig. 6L, M) has a shield's pore density of 15 p/mm^2 and pore diameter of 30–35 μm. It demonstrates two variations of configurations of the funnels in the same specimen with regard to the number and length of postero-lateral extensions. Both funnels have fragments of smooth, large platelet(s) inside.

Specimen **TUG 1025-831** (Fig. 7A). The headshield, where preserved, has a pore density of 13 p/mm^2 and very fine pores (38–48 μm). It was studied in the hope of seeing any endolymphatic structure in the shield's middle layer. Before covering the specimen with gold, the radiating pattern of the left-side structure was weak but perceivable, which nearly disappeared later during the work. The small cap-shaped covering platelet in the middle of the right-side structure has a roundish configuration, a convex surface, and is surrounded by the radial bony network. No pore is seen in that platelet.

Specimen **TUG 1025-358-1** has some places where the remains of both left- and right-side endolymphatic structures can be seen in their basal part of the shield. Their extremities lie in the stone, which is seen around the structure in the SEM pictures. Figure 7B depicts a horizontal cut through the left endolymphatic duct and wall with two (three?) parallel ridges on its anterior side. The duct wall surrounding the lumen is relatively thick.

DISCUSSION

The external endolymphatic structures (otic elevations, funnels, covering platelets, pores in covering platelets; Fig. 2H) have not been studied previously in the osteostracan genus *Tremataspis*. Some data can be found about endolymphatic ducts and openings, the latter having also been referred to as apertures of the endolymphatic ducts (Denison 1947, 1951, p. 162), or endolymphatic pores (Sahney and Wilson 2001; Ladich and Schultz-Mirbach 2016).

The structure of the inner ear of fishes is species-specific and has been studied for many years. However, endolymphatic structures, especially the covering platelets, have not received sufficient attention so far. Below are some possible reasons why.

Firstly, due to their fine dimensions, they were not noticed until SEM studies became the standard in micropalaeontology in the 1980s. Secondly, if the covering platelets were moveable, the connections between them could easily break and the platelets could become damaged or lost after the death of the animal. Thirdly, the preservation of fine covering platelets in horizontally buried headshields was problematic due to the pressure of overlying sediments and compression of the fossils, which might have destroyed or deformed the platelets. Fourthly, as mentioned in *Methods* above, the platelets can be lost during fossil preparation. Fifthly, it is possible that covering platelets are not present in all osteostracan taxa, and further studies will be needed.

Paired endolymphatic ducts are present in all fishes (Maisey 2001), but are not always exposed to the environment. In chondrichthyans, each duct ends at a small external aperture located within the endolymphatic fossa,

Fig. 6. *Tremataspis mammillata* Patten. **A**, **D**, **G**, overall view of the area with endolymphatic structures; **B**, **C**, **E**, **F**, slanting covering platelets in funnels; **H**, small cap-like platelet in a funnel; **I**, dolomite crystals in the funnel; **J**, **K**, oval funnel of the left structure, and concave platelet of the right structure is fixed in the middle of a radial structure; **L**, **M**, morphological variety in the shape of left and right funnels. *Locations:* A–C, TUG 1025-32; D–F, TUG 1030-24; G, H, TUG 1025-840; I, TUG 1025-722; J, K, TUG 1025-728; L, M, TUG 1025-803, Himmiste Quarry; Himmiste Beds of Paadla Regional Stage, Gorstian, Lower Ludlow. Scale bar = 500 μm (A, D, G); 50 μm (B, C, E, F, I, J, L, M); 100 μm (H, K). *Abbreviations:* cap, very small cap-like platelet; cp, covering platelet; dmf, dorsal median field; fix, fixing aid?; wed, wall of endolymphatic duct.
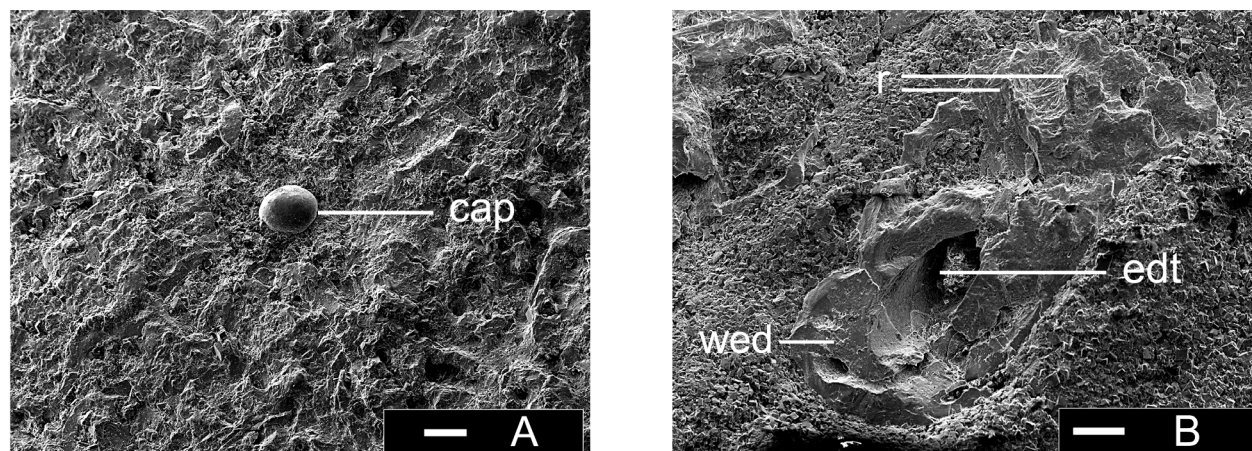
Fig. 7. *Tremataspis mammillata* Patten. Exposed middle layer of the shield. **A**, weakly expressed radial structure with a cap rising higher, TUG 1025-831; **B**, as a result of the breakage of the shield surface layer, the endolymphatic structure with a duct tube, thick wall and ridges on it are exposed. *Locations*: A, TUG 1025-831; B, TUG 1025-358-1, Himmiste Quarry; Himmiste Beds of the Paadla Regional Stage, Gorstian, Lower Ludlow. Scale bar = 100 μm (A, B). *Abbreviations*: cap, very small cap-like plate; edt, endolymphatic duct tube; wed, wall of endolymphatic duct; r, ridges related to the wall.

which is a broad, slightly depressed area on the dorsal surface of the heads of sharks, posterior to the otic capsules (Popper and Fay 1977; Janvier 1996, p. 60). At least some chondrichthyans have an expansion, the endolymphatic sac, partly along the duct (Popper and Fay 1977). However, in bony fishes, the duct ends blindly at the internal endolymphatic sac and may be reduced in many species (Maisey 2001; Ladich and Schultz-Mirbach 2016). In *Synechodus*, the aperture can have a short, narrowing process posteriorly (Janvier 1996, p. 151, fig. 4.40.B2.2, taken from Maisey 1985). The opening in one specimen of *Squalus acanthias* we examined was also slightly comma-shaped but lacked covering platelets or scales. In general, an aperture with a posterior extension might be a similarity among some individuals of *Squalus*, *Synechodus* and *Tremataspis*.

It is noteworthy that all the Silurian osteostracans from the Paleobaltic Basin had external endolymphatic structures postero-lateral to the median dorsal field, while in most osteostracans they open inside that field (Janvier 1996; Sansom 2009). *Procephalaspis* is the only known example from Estonia with corresponding openings at or partly within the postero-lateral corners of that field (Märss et al. 2014, fig. 32A). The reduction of the median dorsal field may have caused the endolymphatic ducts to open outside it (Janvier 1996, p. 107). Our study showed that the position of external endolymphatic structures can vary even within the limits of a single species of *Tremataspis*. They have been found on both sides of the posterior point of the median dorsal field (Fig. 6A), much more anterior to that point on both sides of the field (Fig. 4D), as well as far posterior to it (Fig. 6G).

GIT 846-13, with the superficial layer of the shield and the covering platelets broken away, has an obvious radial structure of the internal bones (Fig. 4I). Such a pattern was well detected in additional specimens before they were coated with gold but disappeared after the coating was applied (Figs 6K, 7A). The horizontal cross-section of the middle layer of the shield at the endolymphatic duct has a radiating appearance in *Tremataspis mammillata*, as shown by Denison (1947, pl. 3, fig. 3) and given herein for comparison (Fig. 8A). Denison (1947, p. 354) found that the sensory canals "converge towards the endolymphatic duct, and appear to dip down into it" and that "the superficial part of the sensory canals is in open connection with the mouth of the duct".

The openings of the endolymphatic duct in *T. mammillata* "contain a number of small plates partly roofing the opening" (Denison 1947, p. 354, fig. 8C), and according to him these "plates" are actually bony processes attached to the basal layer. His figure illustrates the duct and processes in that duct, with the slanting "plates" of *T. mammillata* (Denison 1947, fig. 9B, and re-figured herein in Fig. 8B).

Tremataspis mammillata has one large, slanting covering platelet (Fig. 6B, C), and a small, roundish cap-like platelet for each endolymphatic duct opening (Figs 6H, 7A). The slanting platelets are indeed fixed in the duct, and two examples (Figs 2F right = 6C, and 6E left funnel) confirm it. The other *Tremataspis* species have platelets of different numbers, sizes, configurations, and positions but such fixing structures as in *T. mammillata* have not been detected. *Tremataspis mammillata* differs from the other *Tremataspis* species in several features with regard
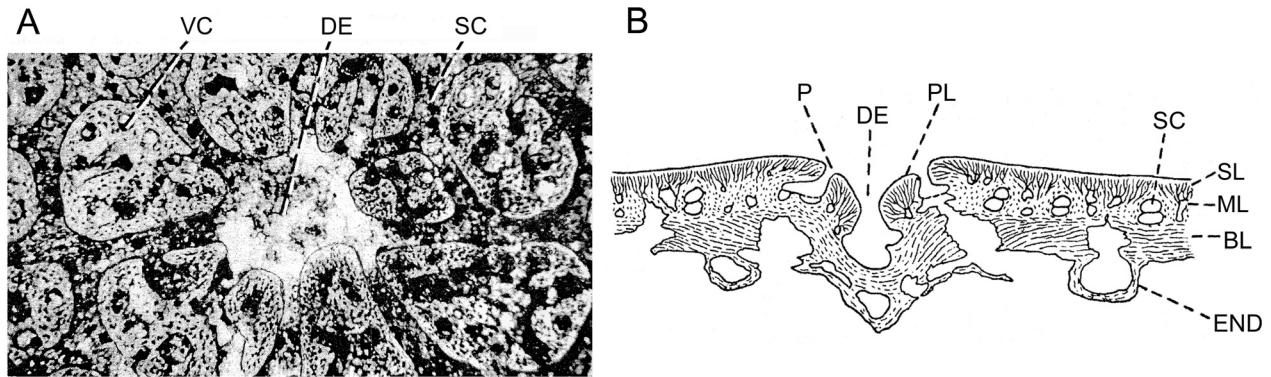
Fig. 8. *Tremataspis mammillata* Patten. **A**, image taken in horizontal view (Denison 1947, pl. 3, fig. 3), and **B**, cross-section of the shield (Denison 1947, fig. 9B).

Denison's abbreviations: BL, basal layer; DE, endolymphatic duct opening; END, endoskeleton; ML, middle layer; P, pore of the sensory canal system; PL, plate or process in the opening of an endolymphatic duct; SC, sensory canal; SL, superficial layer; VC, vascular canal.

to its microstructure (Denison 1947; Märss et al. 2014), which gives reason to think that the endolymphatic structures might also differ in these two groupings. There was a limited time interval for the existence of the five species, with *T. schmidti* being only in the Upper Wenlock, and *T. mammillata* only in the Lower Ludlow, whereas *T. milleri*, *T. perforata* and *T. rohoni* range from the Wenlock to the Ludlow. The time interval between the appearance of *T. schmidti* and that of *T. mammillata* is about 2 million years. Although brief in geologic terms, this amount of time might still be sufficient for the emergence of the altered endolymphatic functions in *T. mammillata*.

We used the nasohypophyseal area, which changes its configuration during ontogeny (Fig. 9A–I), to try to detect possible characters that could be useful for different ontogenetic stages of endolymphatic structures. The bottom and walls separating the nasal and hypophyseal divisions (term from Sansom 2009) are pierced by pores. We recognized three stages from younger to adult. Stage 1– nasal divisions are widely open and have very porous surfaces (Fig. 9A, B); stage 2 – nasal divisions have begun to overgrow starting from the anterior portion (Fig. 9 C–F), and stage 3 – nasal divisions are overgrown, and an oval hypophyseal division occurs inside the oval wall (Fig. 9 G–I). The size of the hypophyseal division does not change very much during development. Figure 9C, F shows no actual opening on the bottom of the nasal divisions. On both sides there is a very distinct sieve with huge pores. We are sure that instead of a single opening, the bottoms of the nasohypophyseal divisions in *Tremataspis* function as sieves. This has not been reported before. There is, in Fig. 9A, C, no good indication of a real opening in the hypophyseal division, although sadly in Fig. 9B, E that part is broken.

When compared to the endolymphatic structures, we admit that there is very little material, but using the specimens at hand, we found only a few specific features suggestive of the developmental stages given above. We noticed, for example, that a thin headshield (e.g., TUG 1025-722, Fig. 6I) has small, roundish funnels. Moreover, small headshields among the specimens of a species from an earlier stage of shield development have smaller pores in the shield (GIT 846-9) and only slightly smaller pores in the covering platelet.

Function of the covering platelets and the funnel

According to Sahney and Wilson (2001, p. 665) "one function of [endolymphatic] openings was... [that] exogenous material enters through the endolymphatic pores and finds its way into the labyrinth of the inner ear". They also suggested that osteostracans possessed a selective mechanism similar to that of extant chondrichthyans, which allows certain grain sizes to enter but excludes others. Agreeing with Sahney and Wilson (ibid.) that the function of this structure was to select the size of the grains before they entered the endolymphatic duct and farther, the way the selection of grain size proceeded in osteostracans is not yet clear.

Tremataspis is one of the few osteostracans in which the endolymphatic openings can be studied in detail. The covering platelets must have helped to limit the maximum size and number of the particles that can enter. Another, not mutually exclusive, possibility is that the platelets might have developed early in ontogeny to frame or fix the size of the openings prior to the ossification of the rest of the shield; however, this is difficult to test because incompletely ossified *Tremataspis* (as in Denison 1947,
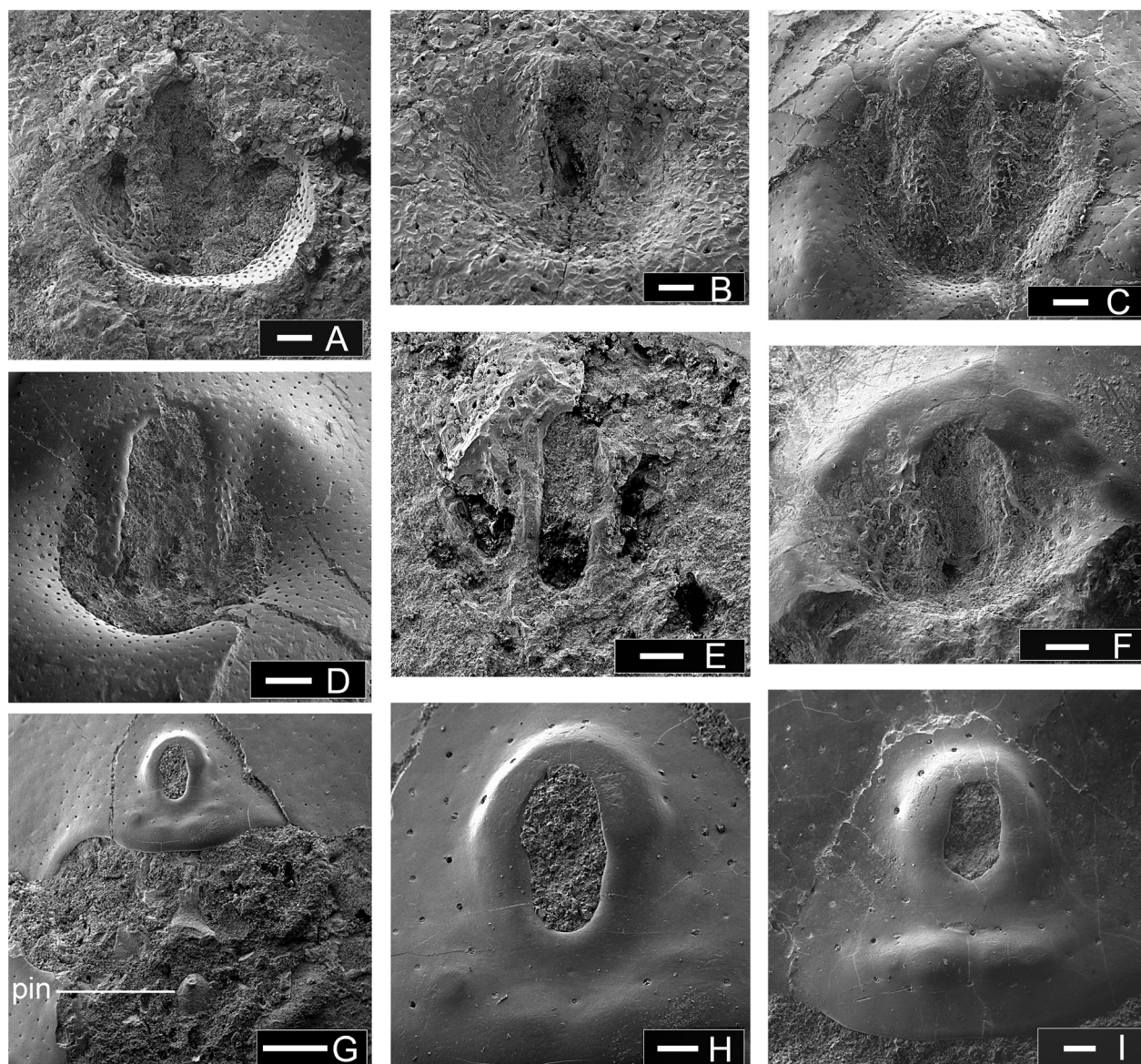
Fig. 9. Nasohypophyseal region of the species of *Tremataspis*. **A–C**, *T. schmidti* Rohon; **D**, *T. milleri* Patten; **E**, *T. rohoni* Robertson; **F–I**, *T. mammillata* Patten. *Locations*: A, GIT 846-9, Elda Cliff, bed II; B, GIT 846-4, Viita Quarry; C, 846-11, Elda Cliff, loose material; D, GIT 846-7; E, GIT 846-10, Elda Cliff, bed IV; F, TUG 1030-27; G= H, TUG 1025-586; I, TUG 1025-803, Himmiste Quarry; Himmiste Beds of Paadla Regional Stage, Gorstian, Lower Ludlow. Scale bar = 200 μm (A–F, H, I), 1 mm (G). *Abbreviations*: pin, pineal structure.

fig. 11) is rare, and a largely unossified *Tremataspis* might not be recognizable in the fossil record. A third possibility is that the individual retained a wider endolymphatic duct opening during initial fulfilling of its need for exogenous grains (otarenae), and then progressively closed down the duct opening by developing more and larger covering platelets.

The shape and size of the endolymphatic duct opening are also of functional interest. One suggestion we have is that the funnel-shaped structure (Fig. 2H) captures more candidate grains than would a simple opening with the same diameter as the duct opening. The funnel then directs these grains into the duct tube itself. Without the funnel-like shape, the chance of capturing grains could be greatly reduced. If the funnel were too large, or if its covering platelets were not sufficiently extensive, the gathered grains would be too many and/or often too large. Thus, the size and shape of the funnel, its role as a funnel, and the configuration of the covering platelets can all be important.

In some extant sharks, grains are thought to enter the duct when the shark is covered in sandy material, for example when the Port Jackson Shark *Heterodontus portusjacksoni* excavates the substrate to find prey (Mills et al. 2011). In that species, the duct can be compressed and then expanded by compressing and expanding the flexible tissue covering the endolymphatic fossa as it is pressed against the sediment. That shark species appears to have no endogenous otoconia, with all its grains being of exogenous origin, according to Mills et al. (2011). In another elasmobranch, *Squatina squatina*, a classic study (Stewart 1906) found no otoconia in the labyrinth but numerous exogenous grains (otarenae) in adults. A late-term unborn pup of the same species had no otoconia in its labyrinth either, so that the individuals must have acquired otarenae after birth. The same study reported that a similar-sized unborn *Squalus acanthias*, in contrast, had numerous otoconia within its saccule.

Since the species of *Tremataspis* were bottom dwellers, the sources of otarenae must have been the local environment. The strata of the Rootsiküla (Wenlock) and Paadla (Ludlow) regional stages of the Paleobaltic (Saaremaa Island localities) represent shallow-water lagoonal and shoal sediments and biota. The sediments of the basin included a wide variety of both carbonates and terrigenous components (Jürgenson 1988). The upper size limit for clay is given as 2 µm, for silt particles the size range is 2–63 µm, and for sand particles it is 63–2000 µm (classification from Sinisalu and Kleesment 2002); this means that both silt and sand grains can be considered as possible candidates for otarenae.

Concerning the rejection of inadequate grains, less dense particles would not function as well as denser ones in terms of hearing and acceleration, and should preferentially be expelled. There are some possibilities as to how this might have occurred.

One possible mechanism for expelling or rejecting grains concerns the otic elevations, which appear to be centered on the openings of the endolymphatic duct and not on the otic capsule. Janvier (1996, fig. 4.16) showed that the entire labyrinth within the otic capsule in *Norselaspis* is positioned much farther anteriorly than the endolymphatic openings. Their precise position suggests that the otic elevations are specifically related to the openings of the endolymphatic duct. Since the elevations are smoothly raised above the surface of the headshield, then it must be the case when the animal is swimming, water passes more quickly over the top of the elevation than near it, creating a lower pressure at the duct opening (similar to the upper surface of an aircraft wing) according to Bernoulli's Principle. The resulting lower pressure might tend to draw out endolymphatic fluid (which is similar to sea water) and any included less dense grains. Whether this effect could have been sufficiently strong to cause significant outflow from the duct is unknown.

Another possibility is, as occurs in some sharks, that small muscles control the walls of the duct (Hanson et al. 1990, fig. 7) and perhaps an enlarged portion of the duct if there is an endolymphatic sac. Contractions of these small muscles could expel grains that are too small or not dense enough to be fully functional (Hanson et al. 1990). Such musculature would require suitable space within the dorsal shield, and evidence for it is still lacking. In summary, mechanisms for expelling grains from the duct are hypothetical and require further study.

Purpose of different pores in the shield of *Tremataspis*

Tremataspis species have differently sized pores in the superficial layer of the headshields (see Tables 2–3), being part of the mucous canal system (Stensiö 1927) or the sensory canal system (Denison 1947).

The sensory canals in the *Tremataspis* headshield are divided into lower and upper parts by a thin, perforated bony septum parallel to the surface (Denison 1947, p. 341, 1966; Bölau 1951; Siebplatten in Gross 1968; Märss et al. 2014; Bremer et al. 2021; sieve plates in O'Shea et al. 2019). The pores of perforated septa are very small, only 1–2 µm. Denison (1947, pp. 350–355) suggested that these septa separated the internal and external parts of the canals while still allowing vibrations and pressure to be transmitted. He further noted that the sensory canals of *Tremataspis* were intimately associated with the openings of the endolymphatic duct, and thus we could propose that the pores surrounding the endolymphatic openings might have a function similar to the pores of the sensory canals.

Why is the left side of a structure unlike the right side of that structure? An example is specimen GIT 502-443 of *T. milleri* (Figs 2B, 4B, C), the species with the largest pores in its covering platelets. The dentated margin is situated toward the lateral side of the headshield and the large pores are toward the midline of the shield. There is no ready explanation for this arrangement. Differences in the presence and size of pores among species raise further questions about their function. If they play an important role, why is it that such pores are absent in *T. mammillata*? If the covering platelets were movable, a wider possible range of grain sizes could enter the duct. Whether they were movable or not, perhaps the pores contained special sensory organs to detect chemicals or minerals passing in or out or into the surrounding environment.

SUMMARY

The complex of external endolymphatic structures in *Tremataspis* is described for the first time. It includes the otic elevation, the funnel and its posterior extensions, the

covering platelets, the opening of the endolymphatic duct within the funnel, and the endolymphatic duct itself. The elements of the structure vary somewhat in different species of the genus, and therefore each structure is species-specific.

The otic elevation is the raised surface of the shield around each of the funnels. The elevation is not directly above the presumed location of the labyrinth or otic capsule, but is rather centered on the endolymphatic opening itself, suggesting a functional relationship. The direction of the longer axis of the elevations copies that of the funnels.

The funnel and duct opening lead into the endo-lymphatic duct tube. The endolymphatic tube and its wall surround the lumen of the duct. The duct tubes narrow with depth and are directed ventrally and anteriorly.

The funnels on the left and right sides of the body can differ considerably from each other in size, configuration, the number of covering platelets, the number and size of the pores in the covering platelet, and dentations at the margins of the shield and covering platelets. The configuration of the funnel can be as an almost perfect ring, or ring-like to ovate, or strongly elongated, but can also be of irregular or complex shape. A small rectangular extension (of the funnel with platelets) is situated posterior to the oval main structure. In the middle of the funnel is an oval or circular endolymphatic duct opening. The funnel accommodates different numbers of covering platelets. Some characteristic features of covering platelets can be pointed out for each species of *Tremataspis*.

Tremataspis schmidti

- Covering platelets have convex surfaces (meaning that no platelet was on top of them);
- Covering platelets are arranged in a wreath-like or circular pattern in one to two parallel sets around the endolymphatic duct opening;
- Covering platelets are usually short, but if not, there is one long platelet on the medial side, and shorter ones on the lateral side;
- Pores in the covering platelets are only slightly larger than those in the shield.

Tremataspis milleri

- Shape and distribution patterns of covering platelets are variable;
- Large covering platelets and large, deep pores are closer to the body midline, while the opposite side is smooth; the platelet's inner margin, close to the duct opening, is dentated;
- Small platelets in one distinct ring or in an oval are around the duct opening;

- The covering platelets can be on one or two levels;
- There are a few pores per covering platelet, or notches, and hooks substituting for pores;
- Posterior or postero-lateral extensions are more common than in any other species;
- The covering platelets, if on two levels and with hooks at the platelet's ends (GIT 846-7, Fig. 4L, M), give the impression that they were movable and had a certain function. The large, oval covering platelets make the endolymphatic opening smaller but do not cover it completely (except seemingly in GIT 846-5, Fig. 4G, J).

Tremataspis rohoni

- Covering platelets are relatively large, and three in number;
- The platelets have smooth and flat surfaces;
- There are only 1–2 pores per covering platelet, or a notch in the middle at the platelet's margin, differing in this respect from *T. mammillata*.

Tremataspis mammillata

- It has the simplest external endolymphatic structures;
- The funnels can be very irregular;
- One smooth, relatively large slanting covering platelet ("bony process" according to Denison 1947) is in each funnel;
- Sloping "platelets" of *T. mammillata* differ from the non-sloping platelets of *T. schmidti*, *T. milleri* and *T. rohoni*;
- A small cap-like roundish covering platelet is relatively frequent;
- Postero-lateral extensions are rather common.

and Gavin F. Hanke, kindly commented on the manuscript and made useful suggestions, thus helping to improve the paper. Nevertheless, all the ideas and descriptions originate from the authors. The publication costs of this article were covered by the Estonian Academy of Sciences.

REFERENCES

Bölau, E. 1951. Das Sinnesliniensystem der Tremataspiden und dessen Beziehungen zu anderen Gefäss-Systemen der Exoskeletts (The sensory line system of tremataspids and its relations to other vascular systems of the exoskeleton). *Acta Zoologica*, **32**(1–2), 31–40 (in German).

Bond, C. E. 1979. *Biology of Fishes*. W. B. Saunders, Philadelphia.

Bremer, O., Qu, Q., Sanchez, S., Märss, T., Fernandez, V. and Blom, H. 2021. The emergence of a complex pore-canal system in the dermal skeleton of *Tremataspis* (Osteostraci). *Journal of Morphology*, **282**(2), 1141–1157.

Chapuis, L. and Collin, S. P. 2022. The auditory system of cartilaginous fishes. *Reviews in Fish Biology and Fisheries*, **32**(2), 521–554. https://doi.org/10.1007/s11160-022-09698-8

Coad, B. W. and McAllister, D. E. 2020. *Dictionary of Ichthyology.* http://www.briancoad.com/dictionary/completedictionary.htm (accessed 2021-08).

Dearden, R. P. and Giles, S. 2021. Diverse stem-chondrichthyan oral structures and evidence for an independently acquired acanthodid dentition. *Royal Society Open Science*, **8**(11), 210822. https://doi.org/10.1098/rsos.210822

Denison, R. H. 1947. The exoskeleton of *Tremataspis*. *American Journal of Science*, **245**(6), 337–365.

Denison, R. H. 1951. Evolution and classification of the Osteostraci. *Fieldiana: Geology*, **11**(3–4), 155–196.

Denison, R. H. 1966. The origin of the lateral-line sensory system. *American Zoologist*, **6**(3), 368–370.

Eichwald, E. 1854. Die Grauwackenschichten von Liv- und Estland (Greywacke layers of Livonia and Estonia). *Bulletin de la Société Impériale des Naturalistes de Moscou*, **27**(1), 1–111 (in German).

Gross, W. 1968. Beobachtungen mit dem Elektronenraster-Auflichtmikroskop an den Siebplatten und dem Isopedin von *Dartmuthia* (Osteostraci) (Observations with the electron scanning reflected light microscope on the sieve plates and the isopedine of Dartmuthia (Osteostraci)). *Paläontologische Zeitschrift*, **42**, 73–82 (in German).

Hanson, M., Westerberg, H. and Öblad, M. 1990. The role of magnetic statoconia in dogfish (*Squalus acanthias*). *Journal of Experimental Biology*, **151**, 205–218.

Janvier, P. 1985. Les thyestidiens (Osteostraci) du Silurien de Saaremaa (Estonie). Première Partie: Morphologie et Anatomie (Thyestiida (Osteostraci) from the Silurian of Saaremaa (Estonia). Part I: Morphology and anatomy). *Annales de Paléontologie*, **71**(3), 83–147 (in French).

Janvier, P. 1996. *Early Vertebrates*. Oxford Monographs on Geology and Geophysics, 33. Clarendon Press, Oxford.

Jürgenson, E. 1988. *Осадконакопление в силуре Прибалтики (Deposition of the Silurian beds in the Baltic)*. Valgus, Tallinn (in Russian).

Kasumyan, A. O. 2004. Vestibular system and sense of equilibrium in fish. *Journal of Ichthyology*, **44** (Supplement 2), S224–S268.

Ladich, F. and Schulz-Mirbach, T. 2016. Diversity in fish auditory systems: One of the riddles of sensory biology. *Frontiers in Ecology and Evolution*, **31**. https://doi.org/10.3389/fevo.2016.00028

Maisey, J. G. 1985. Cranial morphology of the fossil fish elasmobranch *Synechodus dubrisiensis*. *American Museum Novitates*, **2804**, 1–28.

Maisey, J. G. 2001. Remarks on the inner ear of elasmobranchs and its interpretation from skeletal labyrinth morphology. *Journal of Morphology*, **250**(3), 236–264. https://doi.org/10.1002/jmor.1068

Märss, T., Afanassieva, O. and Blom, H. 2014. Biodiversity of the Silurian osteostracans of the East Baltic. *Earth and Environmental Science Transactions of the Royal Society of Edinburgh*, **105**, 73–148. http://dx.doi.org/10.1017/S1755691014000218

Märss, T., Wilson, M. V. H. and Viljus, M. 2022. Species-specific morphology of the endolymphatic openings in the head-shields of the osteostracan genus *Tremataspis* (Agnatha), from the Silurian of Estonia. In *Special Publication of the Ichthyolith Issues: 16th International Symposium on Early and Lower Vertebrates, Valencia, Spain, 20–26 June 2022* (Paredes Aliaga, M. V., Manzanares, E., Mondéjar Fernández, J., Ros Franch, S., Botella, H. and Martínez Pérez, C., eds). University of Valencia, Valencia, **15**, 6.

Mills, M., Rasch, R., Siebeck, U. E. and Collin, S. P. 2011. Exogenous material in the inner ear of the adult Port Jackson shark, *Heterodontus portusjacksoni* (Elasmbranchii). *The Anatomical Record*, **294**(3), 373–378.

Nolf, D. 1985. *Otolithi Piscium. Handbook of Paleoichthyology*, **10**. Gustav Fischer Verlag, Stuttgart.

O'Shea, J., Keating, J. N. and Donoghue, P. C. J. 2019. The dermal skeleton of the jawless vertebrate *Tremataspis mammillata* (Osteostraci, stem-Gnathostomata). *Journal of Morphology*, **280**(7), 999–1025.

Popper, A. N. and Fay, R. R. 1977. Structure and function of the elasmobranch auditory system. *American Zoologist*, **17**, 443–452.

Robertson, G. M. 1938. The Tremataspididae. *American Journal of Science*, Part I, **35**(207), 172–206; Part II, **35**(208), 273–296.

Rojo, A. L. 2017. *Dictionary of Evolutionary Fish Osteology*. CRC Press, Boca Raton,.

Sahney, S. and Wilson, M. V. H. 2001. Extrinsic labyrinth infillings imply open endolymphatic ducts in Lower Devonian osteostracans, acanthodians, and putative chondrichthyans. *Journal of Vertebrate Paleontology*, **21**, 660–669.

Sansom, R. S. 2009. Phylogeny, classification and character polarity of the Osteostraci (Vertebrata). *Journal of Systematic Palaeontology*, **7**(1), 95–115. https://doi.org/10.1017/S1477201908002551

Schnetz, L., Pfaff, C., Libowitzky, E., Johanson, Z., Stepanek, R. and Kriwet, J. 2019. Morphology and evolutionary significance of phosphatic otoliths within the inner ears of cartilaginous fishes (Chondrichthyes). *BMC Evolutionary Biology*, **19**, 238. https://doi.org/10.1186/s12862-019-1568-z

Sinisalu, R. and Kleesment, A. 2002. Purdsetendite granulomeetrilisest klassifikatsioonist (On grain size scale of siliclastic particles). *Bulletin of the Geological Survey of Estonia*, **10**(1), 20–26 (in Estonian).

Stensiö, E. 1927. The Downtonian and Devonian vertebrates of Spitsbergen. Part I. Family Cephalaspidae. *Skrifter om Svalbard og Nordishavet*, **12**, 1–391.

Stensiö, E. 1964. Les Cyclostomes fossiles ou Ostracodermes (The fossils Cyclostomes or Ostracoderms). In *Traité de Paléontologie* (Piveteau, J., ed.). Masson, Paris, **IV**(1), 96–382 (in French).

Stewart, C. 1906. On the membranous labyrinth of *Echinorhinus*, *Cestracion* and *Rhina*. *Zoological Journal of the Linnean Society of London*, **29**(194), 439–442.

Watson, D. M. S. 1937. The acanthodian fishes. *Philosophical Transactions of the Royal Society of London, Series B*, **228**(549), 49–146.

Endolümfaatilised struktuurid Eesti Silurist pärit osteostraakide perekonna *Tremataspis* (Agnatha) peakilpides

Tiiu Märss, Mark V. H. Wilson ja Mart Viljus

Osteostraakide (luukilbiliste) fossiilid Saaremaa Silurist on hästi tuntud juba üle 165 aasta, kuid siiski leidub nende välisskeleti kirjeldamata detaile. Antud artiklis on esmakordselt vaatluse all luukilbiliste perekonna *Tremataspis* nelja liigi endolümfaatilised struktuurid. Iga struktuur sisaldab kuulmekõrgendikku (*otic elevation*), endolümfaatilise toru ava (*endolymphatic duct opening*), lehtrit ava ümber (*funnel*), endolümfaatilise toru kanalit (*endolymphatic duct tube*) ja ava katvaid plaadikesi (*covering platelets*). Nende struktuuride üksikud elemendid moodustavad tunnuste kompleksi iga liigi jaoks, seega on nad liigiomased.